TRANSACTIONS
OF THE AMERICAN FISHERIES SOCIETY

Volume 124 September 1995 Number 5

Transactions of the American Fisheries Society 124:645–662, 1995

Two-Dimensional Hydrodynamic Modeling: A Neglected Tool in the Instream Flow Incremental Methodology

MICHEL LECLERC

Institut National de la Recherche Scientifique (INRS-Eau)
2800 rue Einstein, Suite 105, Quebec, Quebec G1V 4C7, Canada

ANDRÉ BOUDREAULT

Groupe Environnement Shooner Inc.
5355 Boulevard des Gradins, Quebec, Quebec G2J 1C8, Canada

JOSÉ A. BECHARA[1]

Institut National de la Recherche Scientifique (INRS-Eau)

GENEVIÈVE CORFA

Hydro-Québec, Vice-Présidence Environnement
1010 rue St.-Catherine, Montreal, Quebec H2L 2G3, Canada

Abstract.—The instream flow incremental methodology (IFIM) needs to be improved to more reliably predict the effects of altering fish habitat. Two-dimensional (2-D) hydrodynamic modeling with moving boundaries by the finite element approach overcomes may limitations related to classical physical habitat simulation modeling (mostly 1-D). Some of its most important properties are: the spatial resolution of the model can be adapted to the scale of individual fish habitats and to the spatial variability of field data; the areas frequently uncovered because of flow regime are correctly taken into account through the drying–wetting capability; and the flow resistance variables are more accurate in 2-D because they can be specified as functions of the local substrate conditions or lateral shear stresses. This approach is illustrated by a study of the habitat of juvenile Atlantic salmon *Salmo salar* of the Moisie River (Quebec) where a water diversion has been planned. The results of simulations carried out at two sites (a braided reach and a deep, narrow channel) over a wide range of discharges are presented. Average model error was about 10% for velocity and 2% for discharges. A finite element integration procedure allowed habitat suitability indexes (HSI) to be combined with the results of the hydrodynamic model. In this manner, detailed maps of the spatial distribution of the HSI as well as a "weighted usable area" were obtained for each discharge simulated. Atlantic salmon habitat did not appear to be very sensitive to projected flow alterations. The improved accuracy and resolution in predicting the effects of altering physical habitat variables by 2-D models would permit a better understanding of the shortcomings related to biological aspects of IFIM applications.

[1] Present address: Instituto de Limnologia "Dr. R. Ringuelet," C.C. 712, La Plata 1900, Argentina.

Water resource projects (e.g., hydroelectricity, irrigation) often modify river discharge and alter fish habitats, as reflected by rapid changes (hours to days) in water velocity and depth. Substrate and bathymetry may also change but usually over longer periods of time (months to years). These projects may also affect the natural hydrological regime by changing the temporal variability of the discharge and the annual or seasonal water budget.

Physical habitat simulation (PHABSIM or other comparable computer programs) is one of the most widely used methods among the instream flow incremental methodologies (IFIM; Bovee 1978; Morhardt 1986). It has been used to assess the impact of river discharge modifications on fish habitat availability as reflected by the amount of a weighted usable area (WUA). One obtains the WUA by integrating the area of a certain river reach with respect to the local habitat suitability index (HSI) value. The HSI thus reflects the relative suitability of habitat for a particular species. Therefore, WUA can be used in water management to determine a minimum recommended flow for fish habitat conservation.

The PHABSIM method has several limitations with respect to both the physical and biological models (Mathur et al. 1985; Scott and Shirvell 1987; Souchon et al. 1989). For example, when prediction accuracy is low, it is sometimes difficult to determine if the main source of error lies in the physical model, the biological model, or both. Physical variables like depth and mean velocity are usually obtained either from regression analysis of direct field measurements (e.g., discharge against velocity or depth: Milhous et al. 1984) or from oversimplified numerical models (HEC-2, U.S. Army Corps of Engineers; PHABSIM IFG2: Milhous et al. 1984; ENMAG: Killingtveit 1990) that solve a one-dimensional (1-D) energy equation with energy loss from friction as evaluated with Manning's equation. However, a physical characterization strictly based on field measurements and a regression approach is time-consuming because it requires intensive sampling at several discharges (PHABSIM IFG4 computer program: Milhous et al. 1984). Furthermore, it does not permit reliable extrapolations outside of the measured discharge interval. In the physical description by 1-D numerical modeling, relatively crude engineering techniques such as backwater curves and semi-two-dimensional models by discharge corridors have been used (Milhous et al. 1984; Souchon et al. 1989; Heggenes et al. 1994). With these traditional models, reliable results for areas less than 10 m^2 are not easily obtained; hence, the limited data make habitat description difficult at a scale relevant to fish. Moreover, PHABSIM models are sometimes difficult to calibrate (Osborne et al. 1988; Ghanem et al. 1994), and they cannot be easily applied to areas that are frequently uncovered during low-flow periods. Nevertheless, most of the problems related to the physical modeling can be resolved with a full two-dimensional (2-D), vertically integrated approach. Ghanem et al. (1994) compared the two approaches and successfully demonstrated the superiority of the 2-D method, even on data sets typically collected in cross sections for applying a 1-D model. Although 2-D modeling is an engineering tool commonly used to assess effects of flow alteration associated with water resource projects, it has not yet been applied extensively to habitat modeling (Leclerc et al. 1991, 1994).

The main objective of the present paper is to present an application of a 2-D, vertically integrated, hydrodynamic model to predict how fish habitat will be altered. We also present a numerical procedure to compute WUA. This procedure takes advantage of the finite element method and uses physical data provided by the hydrodynamic model. The juvenile populations of Atlantic salmon *Salmo salar* of the Moisie River (Quebec) are used to illustrate the approach.

Study Site

The Moisie River flows into the St. Lawrence Gulf on its northern shore about 20 km west of Sept-Îles, Quebec (50°12'N, 66°05'W; Figure 1). The Moisie River watershed drains an area of 19,248 km^2, which is characterized by a dominant Precambrian bedrock covered by acid soils and a boreal forest dominated by black spruce *Picea mariana,* balsam fir *Abies balsamea* and white birch *Betula papyifera.* The mean annual discharge of the river at its mouth is 436 m^3/s, reaching a maximum in spring and minimum in late winter. The most common fish is the Atlantic salmon, followed by the brook trout *Salvelinus fontinalis.*

Hydro-Québec, a public hydroelectric utility, has undertaken studies on the energy potential of the drainage basin of the Sainte-Marguerite River, a neighbor of the Moisie River. The preliminary planning scheme includes the diversion into the Sainte-Marguerite River of 74% of the discharge of the Aux Pékans River, an upstream tributary of

the Moisie River (Figure 1). This would cause a 42% reduction of the annual average discharge of the Moisie River at the confluence with the Aux Pékans. At the mouth of the Moisie River, the reduction would be 13.4% of the annual average discharge as a result of the additional flow contribution from other downstream tributaries. A major concern of these studies was to determine a minimum recommended flow for preserving Atlantic salmon habitat, which motivated the development and application of the present 2-D model.

Methods of Hydrodynamic Modeling

The main steps of the methodology used in the Moisie River study involved a hydrodynamic model, a biological model (HSI), and a predictive phase integrating the two models (Figure 2). A description of the entire methodological approach is beyond the scope of this paper. Thus, the development of the HSI, as well as some aspects of the predictive phase (hydrological analysis and impact analysis), are considered only briefly. A detailed description of the biological model was given by Boudreault et al. (1989), and the predictive phase was presented by Leclerc et al. (1991).

The objective of the hydrodynamic modeling is to reliably predict the depth, velocity, and wetted surface of river bed over a range of simulated discharges relevant to fish habitat. The technique presented in our paper is the 2-D numerical modeling of free-surface flows by the vertically integrated, shallow-water equations. (A different set of 2-D equations exists to solve laterally integrated flow; this type of model is used to simulate the mean vertical flow patterns associated with density currents and wind-induced flows.) The model presented herein is based on principles of mass and momentum conservation and is solved by finite element algebra (Zienkiewicz 1977; Dhatt and Touzot 1981). This approach, which is a scientifically recognized tool in engineering practice, has been widely applied for more than 20 years to canals, rivers, and estuaries (Brebbia and Partridge 1976; Walters and Cheng 1980; Leclerc et al. 1987, 1990; Hervouet 1992; Ghanem et al. 1994). The present model includes a drying–wetting capability, which allows relatively precise iterative determination of the position of the lateral flow boundaries. However, the precision level relates to grid size and can never be superior to field data density. The location of these boundaries within the model depends on the discharge and is determined during model solving (Leclerc et al. 1990). This property of the model is essential in natural

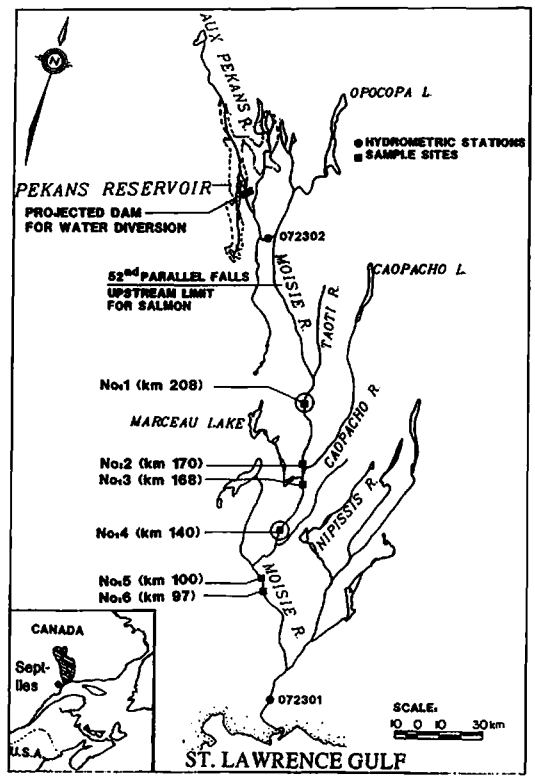

FIGURE 1.—Location of study sites (numbered) along the Moisie River. The inset is the Gulf of St. Lawrence area showing approximate location of Moisie River (shadowed area). See Table 1 for a description of the sites. Stations circled are described in detail in the paper.

systems whose lateral boundary position changes in time, such as rivers and estuaries where the hydrological or tidal regimes may cause significant variations in the wetted surface. A review of models that include drying–wetting capabilities (e.g., Herling 1982; Lynch and Gray 1978; Holtz and Nitsche 1980; Kawahara and Umetsu 1986) was presented by Leclerc et al. (1990). More recently, similar approaches have been made by Zhang et al. (1990), Hervouet (1992), and Ghanem et al. (1994).

Physical Data Collection

Application of the hydrodynamic model involves four main steps, the first of which is data collection (Figure 2). Two sets of physical data are required: first, maps showing bathymetry and dominant riverbed materials for each section of the river being considered, including all areas potentially wetted during floods, and second, reliable stage–discharge relationships at the upstream and

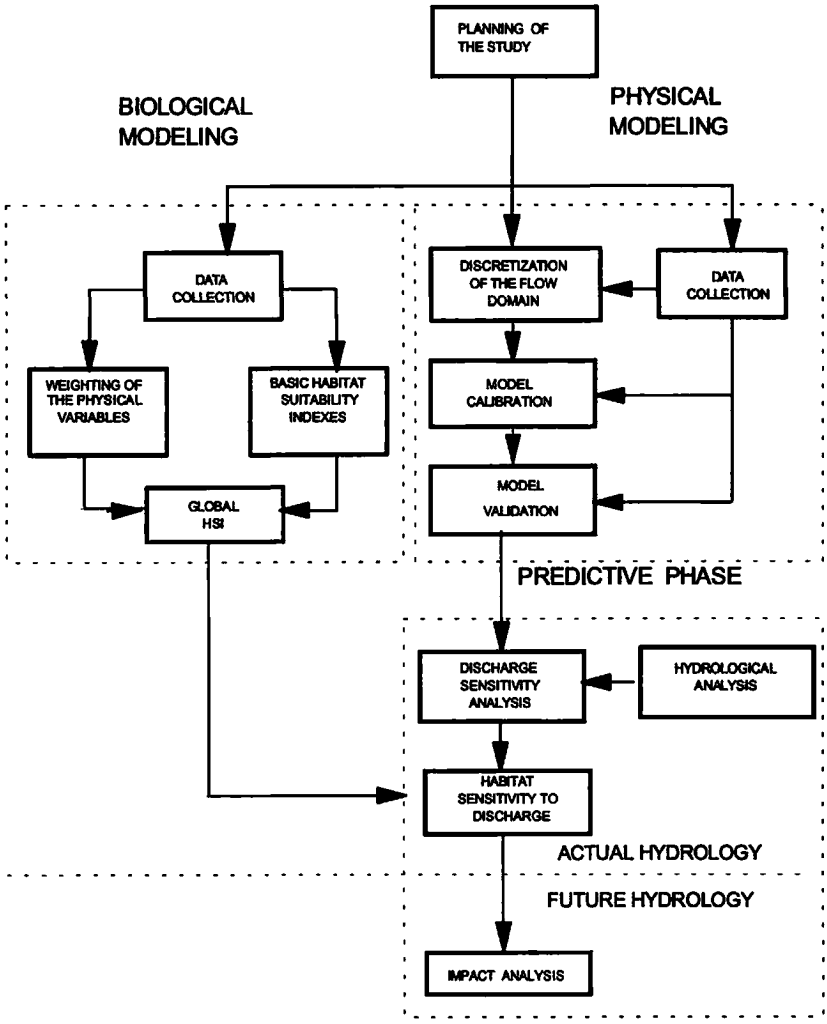

FIGURE 2.—Main steps of the methodology used.

downstream boundaries of the river reach under study. This information is necessary to obtain a good quantitative description of the hydrodynamic behavior of the river reaches where subsequent steps of the model will be applied.

The entire Moisie River was first divided into 25 reaches, which were classified according to their morphological characteristics with aerial photographs (Boudreault 1989). Up to 65% of the Moisie River's length consists of long, deep channel reaches with symmetric or asymmetric flat banks (type A). Shallow, braided reaches (type B) represent 30% of the river. The remaining 5% consists of steep rapids and other rapidly varying flow structures and were not considered in the model's applications. Six reaches, representative of the prevailing river conditions, were then selected for simulation purposes (Figure 1; Table 1). To illustrate model application, only the results corresponding to two sites of contrasting morphological characteristics (one reach of type A and one of type B) are presented and compared here. The results corresponding to the remaining four sites will be used to illustrate model calibration and validation.

To construct the bathymetric and dominant substrate maps for each study site, the so-called "terrain numerical model," bottom levels and substrate sizes were measured in the field. The number of measurement points by unit area within each selected river reach varied from one per 50 m^2 to one per 400 m^2, depending on local heterogeneity

TABLE 1.—Morphometric characteristics and discharges of the sampling sites of the Moisie River.

Sample site[a]	Distance to river mouth (km)	Site length (m)	Summer mean monthly discharge (m^3/s)	Projected reduction of discharge (%)	Reach type[b]
1. Taoti	208	102	198	33	B
2. Caopacho 1	170	425	214	30	A
3. Caopacho 2	168	980	255	25	B
4. Haute-Moisie	140	402	275	22	A
5. Ouapetec	100	192	329	18	AB
6. Eau-Dorée	97	560	330	18	A

[a] The names of the sites were chosen arbitrarily.

[b] A is a long, deep main channel with flat side banks; B is a shallow, braided reach; AB is a reach that combines features of A and B.

of depth and substrate. In the deepest areas, measurements were made systematically along longitudinal transects; in shallow areas, data were collected randomly.

For the calibration reference state, the variables measured were vertically averaged velocity and water surface levels. The number of measurement points per site varied from 11 to 40. The number of data points is much less than that corresponding to bathymetry because in 2-D models, vertically averaged velocity and water level measurements are used mostly for calibration and validation and are not required for solving the model's equations. These measurements are useful at the open boundaries for gauging discharge and establishing the stage–discharge relationship. For numerical modeling, each site should ideally be sampled at three contrasting discharges within the relevant hydrological range of discharge, especially for the stage–discharge relationships. However, a minimum of two distinct events suffices to calibrate and validate the model with respect to velocity and water level.

Because the Moisie River catchment imposed logistical constraints (most study sites were accessible only by helicopter), only upstream and downstream water levels and discharges for at least two distinct events were available for complete validation. Samples for model calibration were taken in July 1987 and July 1988, and samples for model validation were taken in September 1987.

To gauge discharges at the downstream limit of the sites, we divided the transverse section of the river into a number of rectangles and summed the partial discharges calculated for each rectangle (see Hamilton and Bergersen 1984). Relative water surface and bottom levels, as well as the position of each observation point in the x and y spatial coordinates were measured with a Kern theodolite and an electronic distance meter. The mean horizontal velocity over the vertical was calculated from the average velocity near the bottom (0.2 multiplied by total depth) and near the water surface (0.8 multiplied by total depth; Hamilton and Bergersen 1984). Velocity was measured with a Montedoro–Whitney electromagnetic current meter (model PVM-2A). Substrate types near the measurement points were identified by visual examination of the dominant classes of bottom materials. The classes were those from Wentworth (1922) but modified for boulders: large boulders (>100 cm), boulders (100–25 cm), cobbles (25–6.4 cm), pebbles (6.4–3.2 cm), gravel (3.2–0.4 cm), and sand (0.4–0.006 cm). The three most dominant substrate classes at each observation point were noted and assigned a median value. A weighted average grain diameter was calculated for each combination of materials with the following formula:

$$\bar{d} = \sum_{i=1}^{p} w_i d'_i; \qquad (1)$$

$\bar{d}$ is the average grain diameter, d'_i the median value of the ith class, p the number of classes identified at each observation point (maximum of three classes), and w_i the weight used according to the number of classes.

The weights (w_i) used were 0.5 for the first, 0.3 for the second, and 0.2 for the third most dominant classes. When only two classes were present, the weights used were 0.6 and 0.4; and the weight was 1 for the case of a single granulometric category. These weights best represented the prevalence of the different substrate elements.

Governing Equations

The governing equations of mass (discharge) and momentum conservation on which the model is based are the so-called "shallow water equations."

Mass conservation is represented by

$$\frac{\partial h}{\partial t} + \frac{\partial Hu}{\partial x} + \frac{\partial Hv}{\partial y} = 0. \qquad (2)$$

Momentum conservation is represented by

$$\frac{\partial u}{\partial t} + u\frac{\partial u}{\partial x} + v\frac{\partial u}{\partial y} + g\frac{\partial h}{\partial x} = F_x, \qquad (3)$$

$$\frac{\partial v}{\partial t} + u\frac{\partial v}{\partial x} + v\frac{\partial v}{\partial y} + g\frac{\partial h}{\partial y} = F_y, \qquad (4)$$

$$F_x = -\frac{\tau_x}{\rho H} + f_c v + \frac{\partial \tau_{xx}}{\rho \partial x} + \frac{\partial \tau_{xy}}{\rho \partial y} + \frac{C_w \rho_a |W| W_x}{\rho H}, \quad (5)$$

$$F_y = -\frac{\tau_y}{\rho H} + f_c u + \frac{\partial \tau_{yx}}{\rho \partial x} + \frac{\partial \tau_{yy}}{\rho \partial y} + \frac{C_w \rho_a |W| W_y}{\rho H}. \quad (6)$$

Reynolds stresses (with Einstein notation) are

$$\tau_{ij} = \rho \nu_T \left(\frac{\partial u_i}{\partial x_j} + \frac{\partial u_j}{\partial x_i} \right) \qquad \begin{matrix} i = 1, 2 \equiv x, y, \\ j = 1, 2 \equiv x, y. \end{matrix} \quad (7)$$

Bottom friction is represented by

$$\tau_x = -\frac{\rho g n^2 |V| u}{H^{1/3}}$$

and

$$\tau_y = -\frac{\rho g n^2 |V| v}{H^{1/3}}. \quad (8)$$

In these equations, C_w is the wind drag coefficient; F_x and F_y are mass forces along the x and y axes; f_c is the Coriolis coefficient; g is gravity; H is total depth; h is water level; n is Manning's roughness coefficient; t is time; V, u, and v are the vertically integrated velocity module and its x and y components; W, W_x, and W_y are the wind velocity module and its components; ρ is water density; ρ_a is air density; τ_{ij} are Reynolds stresses; τ_x and τ_y are bottom friction in the x and y directions; and ν_T is turbulent viscosity.

The model has two parameters that must be adjusted by calibration: Manning's roughness coefficient (n) and the numerical turbulent viscosity (ν_T) used in computing the Reynolds stresses (Leclerc et al. 1987, 1990). The wind factor (W) was not incorporated in the model simulations because the river runs south in a deep valley, which minimizes the influence of the prevailing westerly winds.

Initial and Boundary Conditions

In this study, steady state conditions were simulated, which did not require special attention to the initial conditions. This implies that the final result for a particular state is independent of the initial conditions. However, the simulation must be sufficiently long to eliminate the errors associated with estimated initial conditions. The initial conditions are usually chosen from the closest hydrological conditions already simulated.

Boundary conditions can be given as discharge, water level, or water velocity. The closed lateral river boundaries were specified as having null tangential and normal velocities (i.e., no slip conditions). Except for two reference states used to calibrate and validate the model, the boundary conditions at the downstream and upstream open sections were specified as actual water levels, and the corresponding discharges were determined by the simulations. With these data, a stage–discharge curve was developed for each site and later compared with field measurements for validation. For a detailed description of the model and application procedures, see Leclerc et al. (1987, 1990).

Discretization

Discretization with the finite element method is a delicate operation that involves dividing the flow domain into a number of triangular elements (Figure 3C, D). Each element was drawn over the bathymetric and dominant substrate map (Figure 3A, B) provided from field data. The size of each element was adapted to represent the morphological variability of the study site. Thus, relatively smaller elements were drawn within areas of rapidly changing bottom morphometry, substrate, or both; this result is referred to as the numerical terrain model (NTM). It is currently possible to use automatic grid generation tools to prepare the NTM readily. At the time of our study, we built the grid by hand, and performed the numerical transformation using a digitizing table.

A six-node triangular element was used in our study (Figure 3D). Bathymetry was specified as a constant property of each corner node. This variable is related to a horizontal datum, and thus it is not the same as depth calculated with respect to a sloping water level. Vertically averaged horizontal velocities were calculated at each of the six nodes, and water levels (and consequently depths) were calculated in the corner nodes of each element. The characteristic substrate was specified as a constant property within each element, so designing each element within homogeneous zones of substrate is important. The algebraic system provided by application of the finite element method to equations (2–7) was solved by the Newton–Raphson method (Dhatt and Touzot 1981). The discretization also allows values of vertically averaged velocity and depth to be produced at any point in the study site by interpolation between the nodes (linear interpolation for water level, depth, and substrate; quadratic interpolation for velocity). The algorithms employed for solving the problem

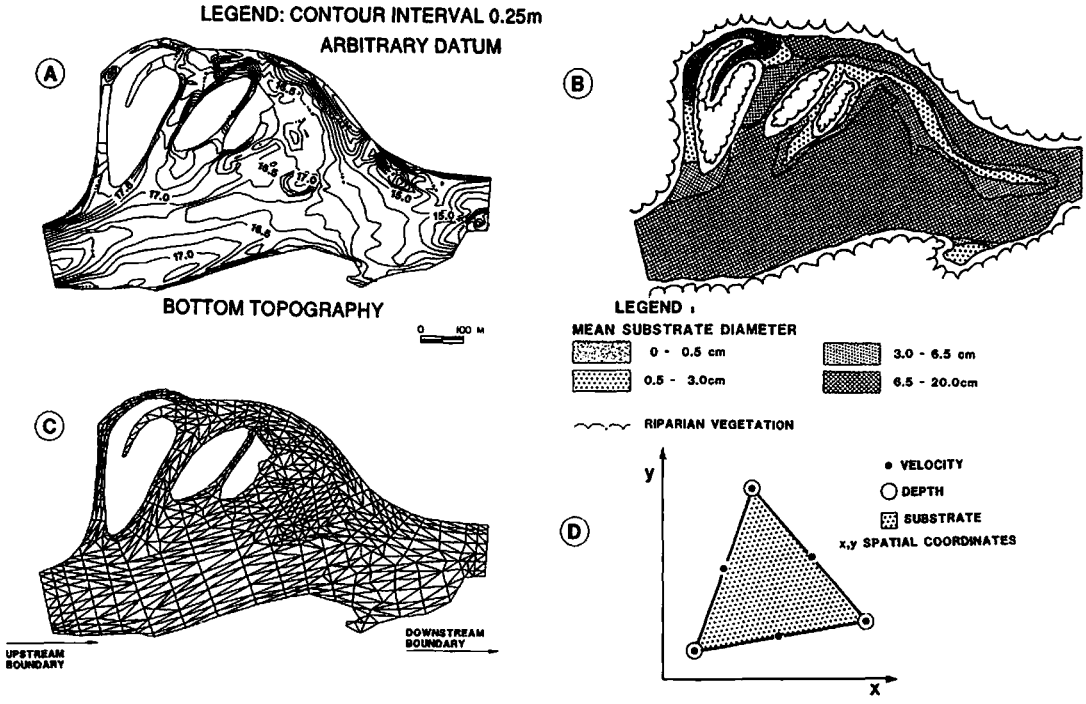

FIGURE 3.—Elements of the Moisie River field model corresponding to site 1 (Taoti): **(A)** bathymetry (topography); **(B)** mean substrate grain size; **(C)** discretized flow domain (hydrodynamic grid); **(D)** six-node element used in the discretization. To facilitate the graphical representation, substrate is shown with a smaller number of categories than actually used in the model. Depths in (A) are in meters relative to a known local reference level.

of drying and wetting areas were described in detail by Leclerc et al. (1990). Note that nodal velocity values were predicted from the simulation model, whereas depths were the difference between predicted water surface levels and measured bottom levels (bathymetry).

Site 1 (Taoti; Figure 3C, D) had a finite element grid of 1,114 elements and 2,382 nodes. Site 4 (Haute-Moisie) had a grid of about 800 elements and 1,700 nodes.

TABLE 2.—Manning's roughness coefficients (n) for riverbed material of different median sizes.

Median substrate size (cm)	Manning's coefficient
0.25	0.02
1.25	0.021–0.024
3	0.023–0.026
6.2	0.03
12	0.028–0.031
16	0.030–0.032
20.5	0.031–0.034
31.5	0.035–0.037
37.5	0.04
44	0.039–0.041
62.5	0.05
87.5	0.05

Model Calibration and Validation

In the present study, the model was calibrated with velocity data from a reference calibration state and the corresponding water levels collected over the entire length of the sites. For the Reynolds stresses, the retained constant turbulent viscosity value varied among sites and was between 3 and 10 m^2/s. For Manning's roughness coefficient, a value for each characteristic bed material size was chosen (Table 2). Most of the substrate of the Moisie River is rather coarse (boulders, cobbles, gravel), yielding stable relationships between roughness coefficients and rugosity. These stable relationships can be explained by the relative stability of materials, which is not the case with fine materials (e.g., sand and silt). The final adjustment of the flow resistance parameter gave a good, stable representation of the discharge, water level, and velocities for all of the modeled reaches.

Ideally, one completely validates the numerical model by comparing simulated and measured wa-

TABLE 3.—Mean errors of the hydrodynamic model simulations for the six Moisie River sample sites.[a] Water level was used for model calibration. Validation for velocities corresponds to the same reference state as that for discharge. These discharges were all higher than mean summer flow so one could calibrate the model everywhere in the flow domain (less dry areas). Validation for discharges includes at least two reference states other than those used for calibration.

Site	Discharge (m^3/s)	Mean error		
		Water level (cm)	Water velocity (%)	Discharge (%)
1	120–188	±3.7 (N = 40)	±14.5 (N = 40)	±2.9 (N = 3)
2	135–260	±3.4 (N = 18)	±9.2 (N = 11)	±2.3 (N = 4)
3	150–308	±2.8 (N = 38)	±5.9 (N = 38)	±0.9 (N = 2)
4	242–319	±3.4 (N = 14)	±9.8 (N = 13)	±1.8 (N = 3)
5	190–280	±3.9 (N = 27)	±7.3 (N = 27)	±4.2 (N = 3)
6	200–390	±3.5 (N = 15)	±11.2 (N = 16)	±0.3 (N = 3)
Global	120–390	±3.4 (N = 152)	±9.7 (N = 145)	±2.1 (N = 18)

[a] N = number of sampling points, $h_e = \frac{1}{N}\sum|h_c - h_m|$, $V_e = \frac{1}{N}\sum\frac{|V_c - V_m|}{V_m}$, and $Q_e = \frac{1}{N}\sum\frac{|Q_c - Q_m|}{Q_m}$; h_e = water level error; V_e = velocity error; Q_e = discharge error; m = measured; c = calculated.

ter levels, velocities, and discharges corresponding to at least two contrasting flow events (the calibration and the validation reference states). Given that water levels and velocities were not available for discharges other than the reference calibration state because of the logistical constraints mentioned earlier, a complete validation of the model was carried out with discharge data. Velocities were validated for the calibration reference state after the model's variables were calibrated with water level data.

Mean differences between measured and calculated water levels, velocities, and discharges were established for the six modeled sites (Table 3). Simulated water levels were within 3.9 cm of observed values. These results are good for the modeled sites, which were between 0.4 to 1.9 km long and whose water levels dropped 60–200 cm within the reach. Simulated water velocities differed from observed values by 6 to 15% which was also good, considering that the model does not take into account certain local hydraulic phenomena (e.g., eddies). Furthermore, 86.3% of the velocity predictions were within 20% of measured values (Table 4). Simulated discharges differed from measured values by less than 5%, which confirmed the adequacy of the simulations for a range of flows between 120 and 390 m^3/s.

TABLE 4.—Frequency distribution of error for water velocity simulations. Data correspond to the 145 sampling points used for calibration of the six modeled sites of the Moisie River. Error was calculated as $V_e = |V_c - V_m|/V_m$ where V_e = velocity error; m is measured and c is calculated.

Error interval (%)	Number of simulated velocities in error interval	Percentage of predicted velocities in error interval
0–10	91	62.8
10–20	34	23.5
20–30	9	6.2
30–40	5	3.5
40–50	3	2.1
50–60	2	1.4
60–70	1	0.7

Methods of Biological Modeling

The mathematical formalism of the biological model is based on the use of nondimensional indexes. The basic indexes consider the single relationships between the abiotic variables of the river and the habitat value for a given life cycle phase of the fish species; the global index, a geometric mean of the basic indexes, integrates the basic influences. Spawning and rearing periods are usually the ones that are considered most sensitive for fishes' survival in rivers.

Habitat Suitability Index

To illustrate our approach, we used the HSIs of the growth phase (June to September) of Atlantic salmon fry (age 0) and parr (ages 1 and 2). These indexes were developed from an intensive sampling effort in three of the modeled sites of the Moisie River (Boudreault et al. 1989). A detailed description of those indexes exists, so only a brief account of the method used to construct them will be presented here.

The indexes were determined for vertically av-

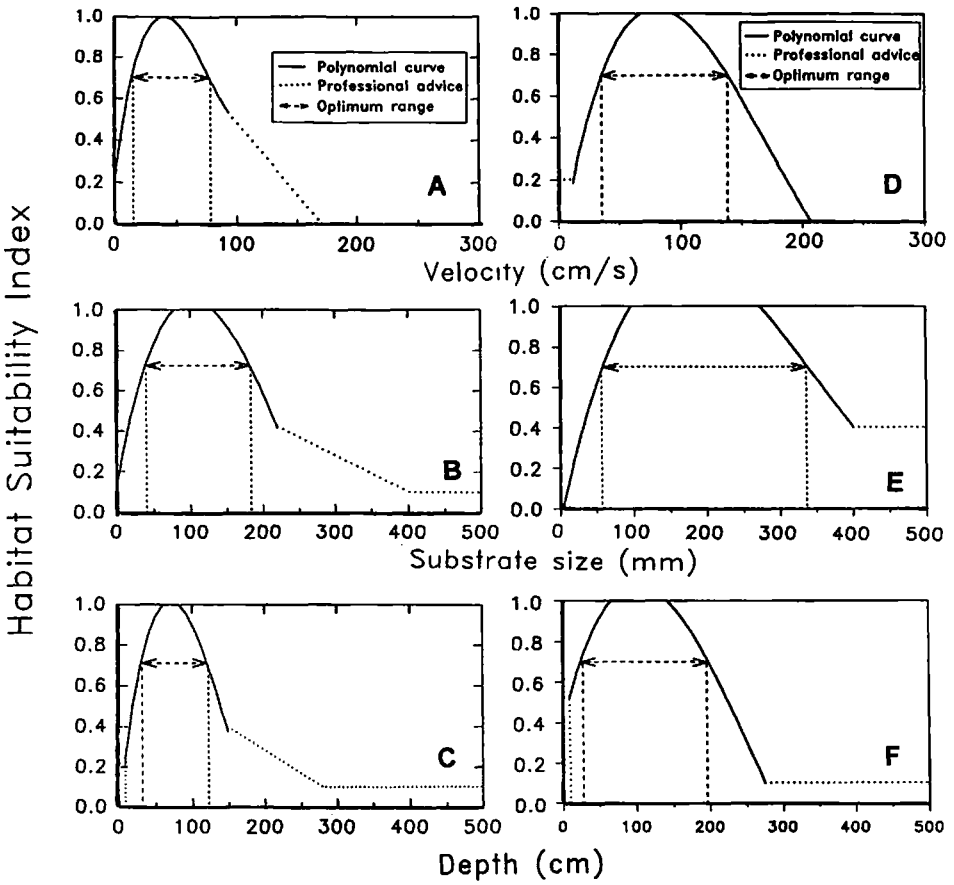

FIGURE 4.—Preference curves for velocity, substrate, and depth for Atlantic salmon fry (A–C) and parr (D–F) in the Moisie River. These curves take into account the availability of physical conditions in the flow domain.

eraged horizontal velocity, depth, and substrate (Figure 4), the first two being strongly related to flow discharge. The resulting curves were empirically established with presence–absence data for the fish populations observed under the natural range of each physical variable. Because our approach accounts for the entire availability of physical conditions, the curves represent habitat preference criteria. The results are curves representing basic indexes (HSI) that vary between 0 and 1 (i.e., complete absence and maximum frequency of fish observed with respect to physical conditions available). These preference curves are often expressed as univariate polynomials resulting from the adjustment of frequency distribution histograms of the presence of fishes with respect to the independent variable (Morhardt 1986).

We then obtained a global index by combining algebraically these basic indexes using a weighted geometric mean approach:

$$I_G = I_1^{a_1} \times I_2^{a_2} \times \ldots \times I_j^{a_j}; \qquad (9)$$

$$\sum_{1}^{N} a_j = 1;$$

I_G is a global index for a given species and a particular life cycle stage; I_j is a basic index (variable j-specific) for the function; a_j is a geometric weight; and j is the total number of abiotic variables considered.

The use of different exponents (a_j) for each habitat variable allowed the basic indexes to be weighted according to their relative importance in defining fish habitat. Weights can be based on a multivariate statistical procedure. In the present study, a principal component analysis was applied (Boudreault et al. 1989). The proportion of the variance among sampling points explained by each variable was used to determine the weights.

After the multivariate statistical analysis, a glob-

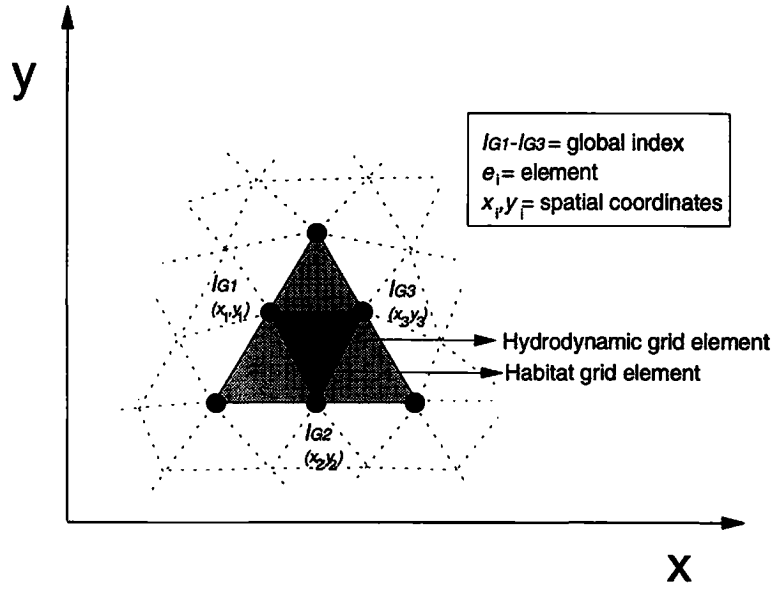

FIGURE 5.—Illustration of the four 3-node elements used for calculating weighted usable area for Atlantic salmon in the Moisie River. Dashed lines represent contiguous elements of the grid.

al HSI was calculated for fry and parr according to the following equations:

$$I_{FG} = I_V^{0.44} \times I_S^{0.3} \times I_D^{0.26} \quad (10)$$

and

$$I_{PG} = I_D^{0.40} \times I_V^{0.39} \times I_S^{0.21}; \quad (11)$$

I_{FG} and I_{PG} are global indexes for fry and parr, and I_V, I_D, and I_S are basic indexes for velocity, depth, and substrate. The most important factor for fry was mean velocity; for parr, depth and velocity were essentially equivalent. Substrate had lower weights, especially for parr.

Calculation of a WUA

Once the hydrodynamic model was calibrated and validated, the next step was integrating it with the biological model to analyze the sensitivity of the habitat to discharge (Figure 2). For each study site, a number of discharges were simulated within a range covering the historical hydrological regime of the river (maximum corresponding approximately to mean annual flood) and the magnitude of the projected reduction in discharge (Table 1). To facilitate calculation of the weighted usable area (WUA), a refined grid was obtained from the subdivision of each quadratically approximated six-node triangular element of the original hydrodynamic grid (Figure 3) in four linear three-node elements as depicted in Figure 5. The physical variables known from the nodal values of the discretized flow model were then transformed to global habitat indexes (I_G) according to equations (10) and (11). Water level values of the midside nodes of the hydrodynamic element were obtained by interpolation from corner nodes. To describe the spatial distribution of HSI, the intervals of the resulting indexes I_G were mapped for an entire study site and for every discharge simulated. The surfaces occupied by different HSI intervals and a global WUA corresponding to the simulated discharge were calculated with a finite element technique of numerical integration. For example, we obtained the WUA for a site by first calculating the WUA^e for each element e, and then summing all the WUA^e of the site. The following formulas were used (see Figure 5 for a better understanding of symbols):

$$\text{WUA}^e = \left(\frac{I_{G1} + I_{G2} + I_{G3}}{3}\right) A^e; \quad (12)$$

$$A^e = \frac{1}{2}[(x_2 - x_1)(y_3 - y_1) - (x_3 - x_1)(y_2 - y_1)]; \quad (13)$$

$$\text{WUA} = \sum_{e=1}^{NE} \text{WUA}^e; \quad (14)$$

WUA^e is the weighted usable area of the eth element; $I_{G1}, \ldots, I_{G3}$ are global indexes for each

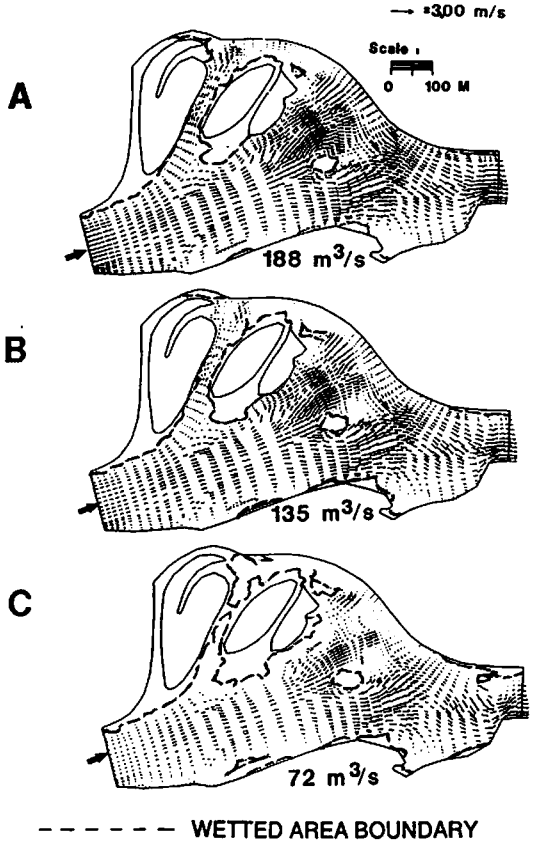

FIGURE 6.—Simulated flow regime for site 1 (Taoti) in the Moisie River at different discharges. Arrows indicate flow direction and (in the crowding of small arrows) intensity.

of the three corner nodes of an habitat element; A^e is area of the element e; x and y are spatial coordinates; and NE, total number of elements of the habitat grid.

Leclerc et al. (1994) described an alternative method for calculating the WUA. It uses a more precise finite element technique involving a higher degree of numerical integration (7 or 12 integration points; see Dhatt and Touzot 1981).

The quality of the habitat was defined arbitrarily according to four usability intervals: 0.0–0.1 = unacceptable; 0.1–0.4 = low acceptability; 0.4–0.7 = medium; and 0.7–1.0 = high. The WUA is expressed as a percentage of the total surface of the study site (percent usable area, PUA), which allows for comparisons among sites having different surfaces:

$$\mathrm{PUA} = 100\frac{\mathrm{WUA}}{A}. \qquad (15)$$

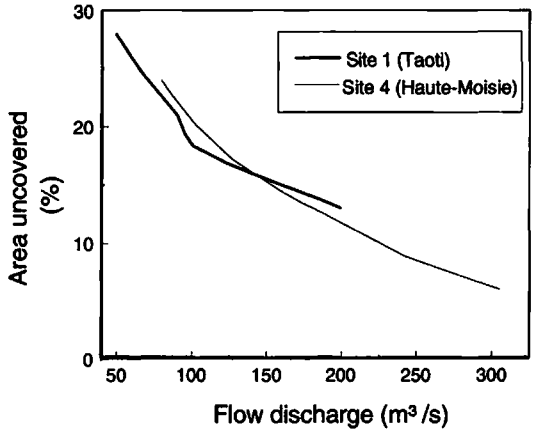

FIGURE 7.—Percentages of uncovered area as function of flow discharge for two studied sites in the Moisie River (100% corresponds to the total area of the modeled flow domain).

Results

Hydrodynamics

Because the hydrodynamics at sites 1 (Taoti) and 4 (Haute-Moisie) were highly similar, only the results for site 1 are presented in detail. Thirty distinct values ranging from 72 to 188 m^3/s were simulated for sensitivity analysis discharge. Flow velocities decreased when discharge was reduced (depicted by the reduced arrow dimensions, Figure 6), but the decrease was not directly proportional to discharge because depth (and consequently the wetted perimeter) was also affected. Thus, at a discharge of 188 m^3/s, maximum velocity reached 1.5–2.2 m/s, but only 1–1.4 m/s at 72 m^3/s.

The decrease in discharge reduced the water level, uncovered more bed, and caused drying (Figures 6, 7). Because of its bed profile, the Taoti reach lost most of its braided structure at the lowest discharges. Site 1 is representative of the most affected reaches within the Moisie River; there the percentage of uncovered area compared to the entire normally flooded area varied from 28% at a discharges of 50 m^3/s to 13% at 200 m^3/s. In contrast, at site 4, the area uncovered varied from 24 to 6% for a larger discharge interval (80–305 m^3/s).

Spatial Distribution of the Habitat Suitability Index

To illustrate the location and changes in usable areas when flow is altered, the global HSI for Atlantic salmon fry at the sites 1 and 4 are presented in Figure 8. At site 1, high-quality areas (I_G =

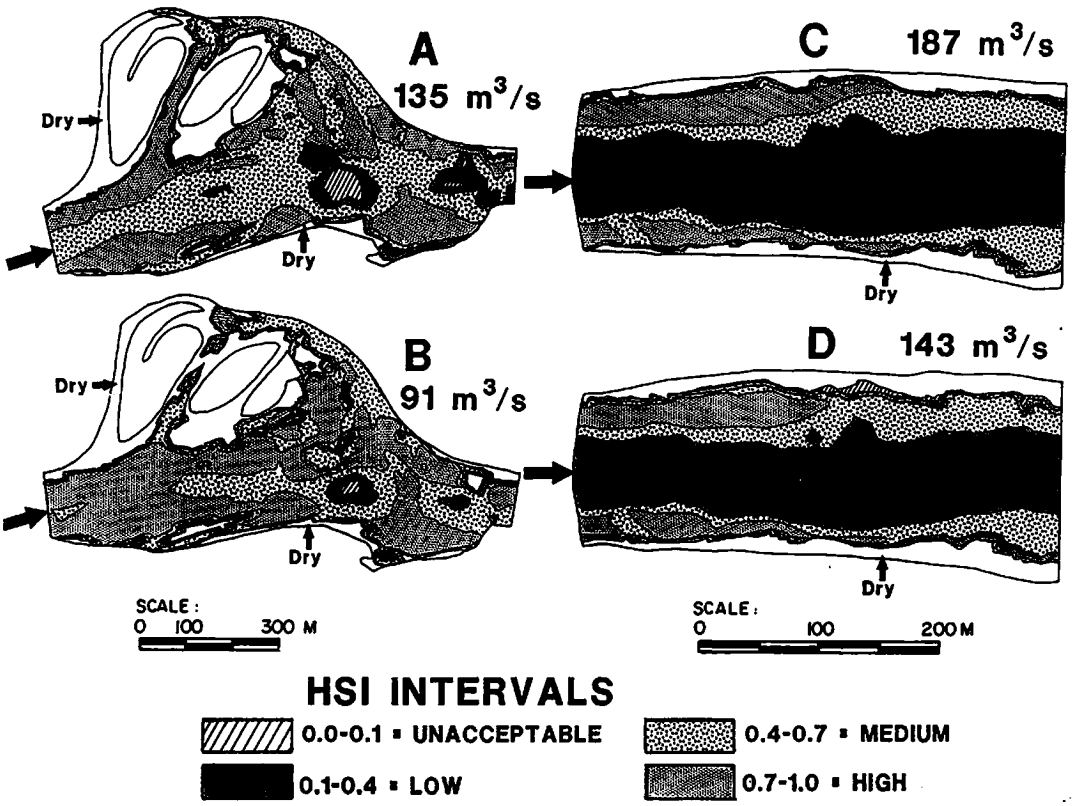

FIGURE 8.—Maps of habitat suitability intervals (HSI) for Atlantic salmon fry (age 0) at different discharges for sites 1 (A, B) and 4 (C, D) in the Moisie River. Big arrows indicate flow direction.

0.7–1.0) shift to the center of the main channel with a reduction in discharge, and their surface areas increase. At site 4, the low-quality areas (I_G = 0.1–0.4) occupy most of the central channel and are compressed with a decrease in discharge. In contrast, the surfaces of the high- and medium-quality areas at site 4 (I_G = 0.4–0.7), limited to the lateral parts of the channel, remain relatively unchanged.

Sensitivity of the Usable Areas

Figures 9 and 10 show the variation in the global HSI intervals and the PUA with discharge for sites 1 and 4. Because the hydrodynamic simulations could not be carried out beyond a certain reliable minimum discharge extrapolated from the stage–discharge relationship, PUA curves are not available in this subrange. However, it is reasonable to state that at a hypothetical zero discharge, the habitat availability would tend to vanish even if still-standing waters remained. Despite the possibility of there being some habitat available at zero-discharge level, its usability would probably be poor and unsustainable. Accordingly, the PUA curves were connected by hand to zero origin with bracketed lines (Figure 9, 10) to make this previous statement more explicit and also to dramatically express the rapid loss of habitat that would arise if upstream diversion significantly reduced flow. However, the exact discharge at which the PUA becomes zero is purely hypothetical and cannot be predicted.

As expected from its type B morphometry, site 1 was the more sensitive to flow reductions of the two samples sites, particularily for parr habitat. A large proportion of that site consists of high- and medium-quality habitats for fry and parr (Figure 9). Any reduction in discharge would be followed by decreases in high-quality habitats for parr and in medium-quality habitats for fry. Thus, the total PUA of parr would decrease more strongly than the total PUA of fry.

Because of its specific shape (type A), site 4 is less sensitive to discharge variations (Figure 10) than site 1. Although this site has lower proportions of high- and medium-quality habitats than

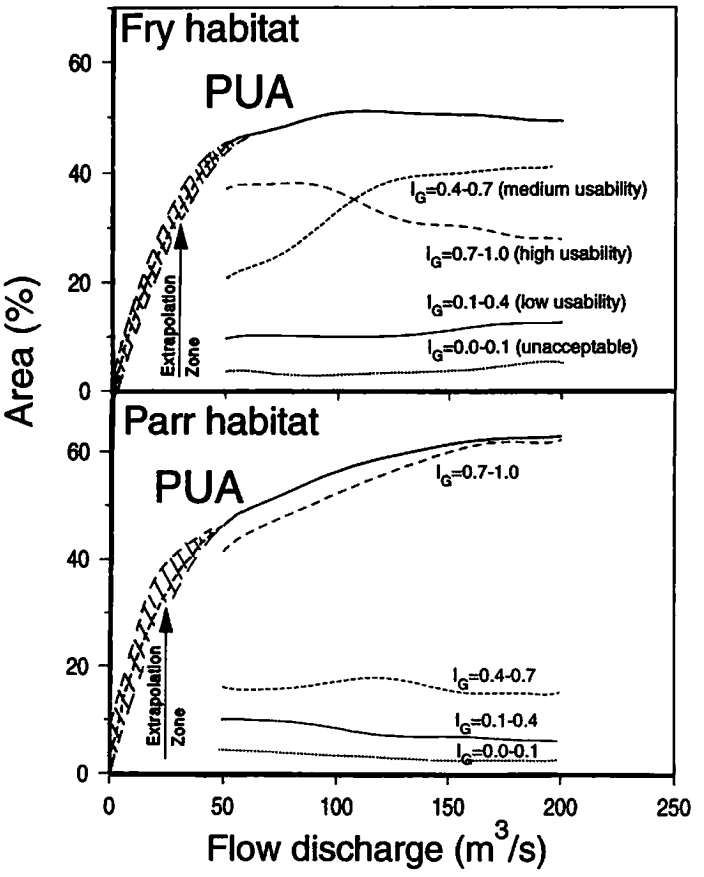

FIGURE 9.—Discharge sensitivity of percentage of usable areas (PUA) and different suitability intervals (I_G) for Atlantic salmon fry and parr habitat for site 1 (Taoti), Moisie River.

site 1, its respective surface areas increased (parr) or decreased only slightly (fry) as discharge declined (Figure 10). Thus, the decrease in PUA for fry and parr was less pronounced than at site 1. However, PUA decreased at the highest discharges simulated, especially for parr.

Discussion

Hydrodynamics

The 2-D numerical approach proposed here has several advantages over traditional PHABSIM methods (i.e., regression analysis, IFG4, and backwater curves, IFG2). The PHABSIM methods are either entirely empirical (IFG4) or take into account only one dimension of flow (IFG2 and IFG4). Therefore, measured velocities and water levels are inputs necessary to generate the results. In contrast, 2-D methods are essentially deterministic, velocity and water levels being model unknowns. Thus, field data on these latter variables are used only to calibrate and validate the model.

It is difficult to compare the two modeling techniques in terms of costs and benefits because different protocols for field data collection are applied to each. The PHABSIM models require subdivision of the reach into a number of individual cells which are determined from transects perpendicular to the river flow (Milhous et al. 1984). This approach has several limitations. Simulation results are restricted to the measurement points previously determined in the transects (Milhous et al. 1984) and are greatly influenced by the number, relative position, and orientation of the transects (Shirvell 1986). Furthermore, these traditional methods assume that velocity and water level do not vary spatially within a cell. This assumption is often not valid, resulting in a frequent source of error in habitat prediction (Shirvell 1987, 1989). In comparison, the 2-D predictive methods that use the finite element approach have simulation points distinct from measurement points. This allows for greater flexibility in choosing the calculation

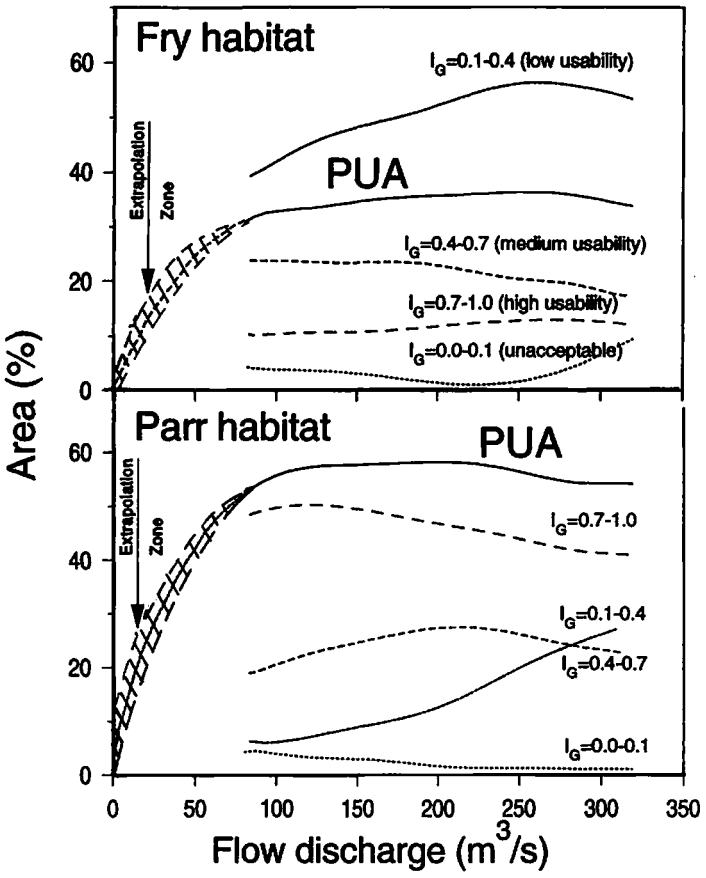

FIGURE 10.—Discharge sensitivity of percentage of usable areas (PUA) and different suitability intervals (I_G) for Atlantic salmon fry and parr habitat for site 4 (Haute-Moisie), Moisie River.

points, for one can adequately place the nodes of the triangular elements during discretization. Furthermore, by using linear or quadratic interpolation among nodes, one can obtain good estimations of velocity fields and water levels for any surface or any point on the modeled site. Given that no single measure of velocity or water level is necessary for discretization, one can concentrate on constructing detailed bathymetric and riverbed material maps, which in turn reduces error in the model's output. Our experience indicates that in rivers having discharges varying from 10 to 1,000 m^3/s, a stratified sampling design, with observation points distributed at densities varying from one per 10 to one per 400 m^2, adequately represents flow conditions.

Because field procedures differed, there were no data available to apply PHABSIM methods to the modeled reaches of the Moisie River; therefore, costs and benefits of the two 2-D models could not be compared. However, to exemplify the field sampling effort required for a PHABSIM application, we estimated the number and types of measurement points necessary to model site 4 (Haute-Moisie). We used a hypothetical data collection strategy similar to that of Shirvell (1989), which corresponds to one sampling point every 70–80 m^2. Site 4 was 402 m long and had a maximum width of 195 m. To construct the 2-D field model, we made 600 measurements of bottom level and substrate on one occasion (one measurement every 131 m^2). Only 14 measurements of water level and 13 of velocity were used to calibrate the model. Complete validation would have required a similar number of measurements at another discharge, thus amounting to 642 items of field data. On the other hand, the minimum sampling effort necessary to implement PHABSIM in the same reach would have required only 20 measurement points per transect (a number frequently used in this kind of modeling (Shirvell 1986). For a cell size of 500 m^2, one transect every 50 m would have sufficed.

To completely calibrate and validate the PHABSIM IFG2 model, a minimum of 200 measurements of velocity, depth, and substrate composition for at least two discharges would have been necessary (total of 1,200 items of field data). For the IFG4 model, data from at least three discharges would have been necessary to obtain reliable adjustments of regression coefficients (minimum of about 1,800 items of data).

Therefore, 2-D models require fewer data and allow a more spatially detailed description of fish habitat than do traditional methods. This feature is particularly useful for studies on territorial fish such as salmonids, which defend territories that rarely exceed 4 m^2 (Grant and Kramer 1990). Moreover, the spatial scale of the model can be changed according to the objectives of the study and available resources by increasing or decreasing the size of each element of the grid during discretization, thereby adapting it to the detail of the bathymetric and riverbed maps available. This capability is useful for those IFIM applications that require detailed habitat descriptions of localized zones within a reach (e.g., up- and downstream faces of spawning areas: Shirvell 1989). With sufficient field data, the adaptative meshing capability of the finite element technique allows for more detailed physical description of any area within a reach which can be accomplished by reducing the size of the elements within those areas.

Another advantage of the 2-D models is enhanced accuracy in estimating the physical variables provided by a better representation of the field data and greater reliability in calibrating Manning's roughness coefficients. These variables can be adjusted at each of the nodes according to the local type of substrate. As pointed out by Ghanem et al. (1994), the 2-D models do not consider the river as a number of independent cross sections but as a spatial continuum. Consequently, the accuracy of results is relatively high, as evidenced by the low mean error in discharge simulations (2.1%). The mean error for discharges reported for 10 PHABSIM applications with one calibration point varied between 19 and 39%, depending on the extent of extrapolation from the calibration flow (Bovee and Milhous 1978). The mean error of 9.7% for velocities reported in our paper is common to other 2-D model applications (Leclerc et al. 1987, 1990, 1994). Our results on the frequency distribution of error for velocity simulations also compare favorably with those reported by Bovee and Milhous (1978) for the PHABSIM IFG4 method. Moreover, estimates for velocity error were carried out with very localized measurement points, indicating that an important proportion of the observed error can be attributed to local aspects of the flow (e.g., eddies) and to field measurement inaccuracies. However, additional measurements at different discharges in the modeled sites of the Moisie River are necessary to completely validate the model for velocities and water levels.

The capacity of 2-D numerical modeling to correctly simulate flow conditions for areas frequently uncovered is another advantage over the classical numerical methods. That property results from the particularity of the numerical procedure employed (Leclerc et al. 1990). A common source of error in traditional methods for low-gradient areas is the assumption of a constant Manning's coefficient for each of the individual transects or cells into which a given river section is divided (Milhous et al. 1984). However, Manning's coefficient must change when some of these cells or transects are partially uncovered. This situation is aggravated because some channel segments may be out of the water when the calibration is made, making adjustment of Manning's coefficients impossible. The 2-D method used does not solve some other problems related to the Manning's coefficient. For example, the technique does not consider changes in sediment composition with a reduction in discharge. Given the large size of the Moisie River sediments, a reduction in the spring flood peaks probably would increase accumulation of fine sediments during low-flow periods and reduce resuspension. Also, when substrate elements like boulders or cobbles occupy a substantial proportion of the water column the value of Manning's coefficient can change with flow. Thus, the 2-D model is not recommended for shallow rivers and small streams (flows of less than 25–50 m^3/s) having large, rocky substrata, because the relative importance of bottom particle size in these cases requires adjusting Manning's coefficient for different discharges.

Despite its advantages, we did not find in the literature any other application of 2-D numerical modeling by finite elements to describe biological habitats. A notable exception is Ghanem et al. (1994) who have only proposed to use this approach. Its lack of use probably results from disciplinary barriers and its apparent mathematical complexity. However, with the arrival of high-powered and affordable personal computers, some of these problems can be surmounted. Some commercial computer programs for hydrodynamic simulations in civil engineering are already avail-

able (e.g., TELEMAC: Hervouet 1992). In addition, most university departments of civil engineering or environmental science have at least one or two homemade computer programs of this type available.

Nevertheless, the complexity of the mathematical approach remains a challenge that requires the collaboration of multidisciplinary research groups, involving hydraulic engineers, biologists, and fisheries managers. In this sense, that type of analysis is very close to the hydrological approach used to evaluate the energetic potential of a river as well as to design civil works, and is therefore well understood by specialists (usually engineers) involved in planning and managing hydroelectric power installations. Because it facilitates multidisciplinary communication among various specialists, the approach can be highly useful in assessing different scenarios during technical negotiations on the minimum flow to maintain in the river network.

Habitat Sensitivity to Discharge

Application of the 2-D model to habitat analysis of the two Moisie River sites illustrates model flexibility for river reaches having different morphological characteristics. In general, the results show that the PUA was not very sensitive to large variations in discharge within the simulated range, perhaps because this range was too narrow. An exception was the parr habitat at site 1 (Taoti) which was more sensitive to lower discharge than at site 4. Most of the Taoti reach is composed of very good habitat for parr. Thus, predicted habitat losses resulted from pronounced reduction in the wetted surface, as well as from changes in habitat quality with flow. At site 4, only the location of the various suitability intervals showed a strong sensitivity to variation in discharge; the zones closer to the main channel became more acceptable as discharge decreased. This gain in physical habitat fully compensated for the losses associated with any narrowing of the wetted section. As a result, the PUA tended to increase with decreased discharge. This agrees with the conclusions of Mosley (1982) and Glova and Duncan (1985), who found that reduced discharge may enhance physical habitat availability. However, these conclusions are more applicable to river reaches with a deep main channel and a swift current, the type of reach that is most common in the Moisie River.

The spatial resolution of the finite element approach is open to many other promising applications in fish habitat modeling. For example, the location and changes in usable areas can be tracked so that the distance and velocity of habitat displacement can be measured after changes in discharge. This property was used by Leclerc et al. (1994) to quantify the stability of fish habitat in rivers exposed to peaking exploitation regimes.

In our study, PUA values were obtained with HSIs for averaged vertical velocity at the fish's position. However, an HSI corresponding to any distance from the riverbed could eventually be approximated with a vertical velocity profile. One can obtain this profile at each node by calculating a logarithmic velocity distribution using depth, substrate roughness, and simulated mean velocity (Yalin 1977). Numerical interpolation could then be used to reconstruct a semi-3-D velocity field to which to apply HSI corresponding to velocities at the depth occupied by the fish (nose velocity).

Conclusions

Two-dimensional modeling by the finite element method is a technique that can be readily used in IFIM applications, because it offers the advantages of high spatial resolution, drying–wetting capacity, reduced error, and reliable calibration and validation. The results of our hydrodynamic modeling approach can be easily transformed to habitat values in terms of WUA or HSI intervals with finite element calculation techniques. This modeling approach is not intended to solve all of the limitations related to hydrodynamics, such as the temporal variability in bathymetry and Manning's coefficient. Therefore, it is best adapted to the modeling of medium to large rivers. It has higher predictive capacity than IFIM, improves the prediction of the hydrodynamic variables, and better permits identification of errors caused by inaccuracies in the biological models (HSI).

Acknowledgments

We are grateful to the following members of the expert committee, who assisted with helpful suggestions that improved the research program: Alek Bielak, Mike Chadwick, Yvon Coté, Marc Drouin, Karl Schiefer, and Gaétan Hayeur, chairman. We also thank Paul Boudreau for the critical revision of an early version of the manuscript, and Jean-François Bellemare for the implementation of the hydrodynamic model. Gilles Tremblay, Louis Belzile, and Pierre Berubé provided valuable support during field sampling. Finally, we acknowledge the Vice-Présidence Environnement of Hydro-Québec for their financial support and for authorizing the publication of the results.

References

Boudreault, A. 1989. Analyse de la représentativité des tronçons utilisés pour la modélisation en 1987 et 1988 par rapport à l'ensemble du cours principal de la Moisie. Report of Gilles Shooner et Associés to the Direction de l'Environnement d'Hydro-Québec, Quebec City.

Boudreault, A., M. Leclerc, J. F. Bellemare, and G. Shooner. 1989. Étude des répercussions du détournement de la rivière Aux Pékans sur les habitats salmonicoles de la rivière Moisie. Report of Gilles Shooner et Associés to the Direction de l'Environnement d'Hydro-Quebec, Quebec City.

Bovee, K. D. 1978. The incremental method of assessing habitat potential for coolwater species, with management implications. American Fisheries Society Special Publication 11:340–346.

Bovee, K. D., and R. Milhous. 1978. Hydraulic simulation in instream flow studies: theory and techniques. U.S. Fish and Wildlife Service FWS/OBS-78/33.

Brebbia, C. A., and P. Partridge. 1976. Finite element models for circulation studies. Pages 141–159 *in* C. A. Brebbia, editor. Mathematical models for environmental problems. Pentech Press, London.

Dhatt, G., and G. Touzot. 1981. Une présentation de la méthode des éléments finis. Maloine, Paris.

Ghanem, A., P. Steffler, F. Hicks, and C. Katopodis. 1994. Two-dimensional finite element flow modeling of physical fish habitat. Pages 84–89 *in* Proceeding of the 1st International Association for Hydraulic Research Symposium on Habitat Hydraulics. Norwegian Institute of Technology, Trondheim, Norway.

Glova, G. J., and M. J. Duncan. 1985. Potential effects of reduced flows on fish habitats in a large braided river, New Zealand. Transactions of the American Fisheries Society 114:165–181.

Grant, J. W., and D. L. Kramer. 1990. Territory size as a predictor of the upper limit to population density of juvenile salmonids in streams. Canadian Journal of Fisheries and Aquatic Sciences 47:1724–1737.

Hamilton, K., and E. Bergersen. 1984. Methods to estimate aquatic habitat variables. Report of Colorado Cooperative Fishery Research Unit to the U.S. Bureau of Reclamation, Engineering and Research Center, Denver, Colorado.

Heggenes, J., S. J. Saltveit, K. A. Vaskinn, and O. Lingaas. 1994. Predicting fish habitat use response in waterflow regime: modeling critical minimum flows for Atlantic salmon, *Salmo salar,* and brown trout, *S. trutta,* in a heterogeneous stream. Pages 124–142 *in* Proceeding of the 1st International Association for Hydraulic Research Symposium on Habitat Hydraulics. Norwegian Institute of Technology, Trondheim, Norway.

Herling, B. 1982. Coupling of one- and two-dimensional finite elements for the computation of tidal flows in estuaries. Advances in Water Resources 5(4):227–232.

Hervouet, J. M. 1992. Solving shallow water equations with rapid flows and tidal flats. Pages 537–548 *in* W. R. Blain and E. Cabrera, editors. Hydraulic engineering software 4. Fluid flow modelling. Elsevier Applied Science, London.

Holtz, K. P., and G. Nitsche. 1980. Tidal wave analysis for estuaries with intertidal flats. Pages 5.113–5.126 *in* S. Y. Wang, C. V. Alonso, C. A. Brebbia, W. G. Gray, and G. F. Pinder, editors. Proceedings of the third international conference on finite elements in water resources. University of Mississippi Press, Oxford.

Kawahara, M., and T. Umetsu. 1986. Finite element method for moving boundary problems in river flows. International Journal of Numerical Methods in Fluids 6:365–386.

Killingtveit, A. 1990. ENMAG user's manual. University of Trondheim, Trondheim, Norway.

Leclerc, M., J. F. Bellemare, G. Dumas, and G. Dhatt. 1990. A finite element model of estuarian and river flows with moving boundaries. Advances in Water Resources 13(4):158–168.

Leclerc, M., B. Bobée, A. Boudreault, G. Shooner, and G. Corfa. 1991. Instream flow incremental methodology and 2-D hydrodynamic modeling: efficient tools to determine guaranteed minimum flow for biological purposes. Pages 289–300 *in* D. Ouazar, D. Ben Sari, and C. A. Brebbia, editors. Computer methods in water resources 2: computational hydraulics and hydrology. Proceedings of the second international conference, Marrakesh, Morocco. Springer-Verlag, Berlin.

Leclerc, M., P. Boudreau, J. Bechara, and G. Corfa. 1994. Modélisation de la dynamique de l'habitat des ounaniches (*Salmo salar*) juvéniles de la rivière Ashuapmushuan (Québec, Canada). Bulletin Français de la Pêche et de la Pisciculture 332:11–32.

Leclerc, M., and six coauthors. 1987. Modélisation des écoulements de l'Archipel de Montréal par élements finis: aspects divers de l'application. Revue Internationale des Sciences de l'Eau 3(2):41–56.

Lynch, D. R., and W. G. Gray. 1978. Finite simulation of shallow water problems with moving boundaries. Pages 2.23–2.42 *in* C. A. Brebbia, W. G. Gray, and G. F. Pinder, editors. Proceedings of the second international conference on finite elements in water resources. Pentech Press, London.

Mathur, D., W. H. Bason, E. D. Purdy Jr., and C. A. Silver. 1985. A critique of the instream flow incremental methodology. Canadian Journal of Fisheries and Aquatic Sciences 42:825–831.

Milhous, R., D. L. Wegner, and T. Waddle. 1984. User's guide to the physical habitat simulation system (PHABSIM). U.S. Fish and Wildlife Service FWS/OBS-81/43.

Morhardt, J. E. 1986. Instream flow methodologies. Report of EA Engineering, Science and Technology, Inc. to Electric Power Research Institute, Palo Alto, California.

Mosley, M. P. 1982. The highs and lows of braided rivers. Soil and Water 18:22–23.

Osborne, L. L., M. J. Wiley, and R. W. Larimore. 1988. Assessment of water surface profile model: accu-

racy of predicted instream fish habitat conditions in low-gradient, warmwater streams. Regulated Rivers: Research and Management 2:619–631.

Scott, D., and C. S. Shirvell. 1987. A critique of the instream flow incremental methodology and observations on flow determination in New Zealand. Pages 27–43 *in* J. F. Craig and J. B. Kemper, editors. Regulated streams. Advances in ecology. Plenum Press, New York.

Shirvell, C. S. 1986. Pitfalls of physical habitat simulation in the instream flow incremental methodology. Canadian Technical Report of Fisheries and Aquatic Sciences 1460.

Shirvell, C. S. 1989. Ability of PHABSIM to predict chinook salmon spawning habitat. Regulated Rivers: Research and Management 3:277–289.

Souchon, Y., F. Trocherie, E. Fragnoud, and C. Lacombe. 1989. Les modèles numériques des microhabitats des poissons: application et nouveaux développements. Revue des Sciences de l'Eau 2:807–830.

Walters, R. A., and R. T. Cheng. 1980. Accuracy of an estuarine hydrodynamic model using smooth elements. Water Resources Research 16(1):187–195.

Wentworth, C. K. 1922. The shape of pebbles. U.S. Geological Survey Bulletin 730-C:19–114.

Yalin, M. S. 1977. Mechanics of sediment transport, 2nd edition. Pergamon Press, Oxford, UK.

Zhang, B. N., F. Bouttes, and G. Dhatt. 1990. A shallow water finite element model for moving fronts. *In* G. Gambolati, A. Rinaldo, C. A. Brebbia, W. G. Gray, and G. F. Pinder, editors. Proceedings of the eighth international conference on computational methods in water resources. Venice, Italy.

Zienkiewicz, O. C. 1977. The finite element method, 3rd edition. McGraw-Hill, London.

Received October 7, 1992
Accepted February 17, 1995